β-delayed neutron emission from ^{85}Ga

K. Miernik,[1,*] K. P. Rykaczewski,[2] R. Grzywacz,[2,3,4] C. J. Gross,[2] M. Madurga,[3] D. Miller,[3] D. W. Stracener,[2] J. C. Batchelder,[5] N. T. Brewer,[6] A. Korgul,[1] C. Mazzocchi,[1] A. J. Mendez II,[7] Y. Liu,[2] S. V. Paulauskas,[3] J. A. Winger,[8] M. Wolińska-Cichocka,[2,4,9] and E. F. Zganjar[10]

[1] *Faculty of Physics, University of Warsaw, Warsaw PL-02-093, Poland*
[2] *Physics Division, Oak Ridge National Laboratory, Oak Ridge, Tennessee 37831, USA*
[3] *Department of Physics and Astronomy, University of Tennessee, Knoxville, Tennessee 37996, USA*
[4] *Joint Institute for Nuclear Physics and Application, Oak Ridge, Tennessee 37831, USA*
[5] *Department of Nuclear Engineering, University of California, Berkeley, Berkeley, California 94702, USA*
[6] *Department of Physics and Astronomy, Vanderbilt University, Nashville, Tennessee 37235, USA*
[7] *Department of Chemistry and Physics, Campbell University, Buies Creek, North Carolina 27506, USA*
[8] *Department of Physics and Astronomy, Mississippi State University, Mississippi 39762, USA*
[9] *Heavy Ion Laboratory, University of Warsaw, Warsaw PL-02-093, Poland*
[10] *Department of Physics and Astronomy, Louisiana State University, Baton Rouge, Louisiana 70803, USA*

(Received 24 February 2018; revised manuscript received 18 April 2018; published 15 May 2018)

Decay of ^{85}Ga was studied by means of β-neutron-γ spectroscopy. A pure beam of ^{85}Ga was produced at the Holifield Radioactive Ion Beam Facility using a resonance ionization laser ion source and a high-resolution electromagnetic separator. The β-delayed neutron emission probability was measured for the first time, yielding 70(5)%. An upper limit of 0.1% for β-delayed two-neutron emission was also experimentally established for the first time. A detailed decay scheme including absolute γ-ray intensities was obtained. Results are compared with theoretical β-delayed emission models.

DOI: 10.1103/PhysRevC.97.054317

I. INTRODUCTION

One of the most basic methods for experimental studies of exotic nuclei is based on decay spectroscopy. For neutron-rich isotopes the main decay branch is the β^- transmutation. Typically, after β decay the daughter nucleus is in an excited state which subsequently deexcites by γ-ray emission. However, with a growing number of neutrons and increasing β-decay energy (Q_β), the decay may feed states which are beyond the neutron separation energy (S_n) of the decay daughter. As a consequence, a new decay channel emerges—β-delayed neutron emission (βn)—which competes with de-excitation by γ-ray emission.

From the point of view of nuclear structure, the β decay can supply information in two ways. The excited states, populated in the decay, emit γ rays. Energies and connections of transitions into cascades allows us to precisely determine the structure of the decay daughter. The observed feeding of the states allows us to partially determine spins and parities of states, based on angular-momentum selectivity of β decay. The drawback of this method is vulnerability to the so-called pandemonium effect [1]. The β feeding, at high excitation energies, tends to be fragmented between many states and most of the emitted weak γ ray may remain undetected, as the efficiency of typical high-resolution germanium detectors is very low for high-energy γ rays. As a result, the picture of the β-strength function obtained by studies of γ-ray balances may be significantly distorted. In order to take into account possible impact of this effect, it is important to measure the absolute intensities of the emitted γ rays. This allows establishing the amount of "missing" γ radiation, and setting realistic limits on the apparent β feedings.

On the other hand, the delayed neutron emission probability (P_n) and the half-life ($T_{1/2}$) are the two most basic parameters of β decay that depend on the integrated quantities of nuclear structure. $T_{1/2}$ provides information on a integrated total strength function, whereas P_n probes the part of the strength function above the neutron separation energy. Therefore, experimental measurement of these values often provides a first insight into the nuclear structure.

In the chain of gallium isotopes, the half-lives and P_n values for neutron-rich nuclides are currently known up to ^{86}Ga, with the exception of a P_n value for ^{85}Ga [2,3]. In this article we address this gap. The data presented here were partially used in the analysis of the β-delayed two-neutron decay of ^{86}Ga [3]. Particularly, it was crucial to determine the γ ray emitted after the β-delayed one-neutron emission from ^{85}Ga, and show its correspondence to the γ ray emitted after β-delayed two-neutron emission from ^{86}Ga. In this article, however, we are focused on a detailed analysis of β decay of ^{85}Ga, including first experimental determination of the P_n value, and obtaining very important information on absolute

*kmiernik@fuw.edu.pl

branching ratios for γ rays emitted in this decay and in decay of ^{85}Ga daughters.

It is worth noticing that neutron-rich $^{83–87}$Ga isotopes are predicted to lie on the path of the astrophysical rapid neutron capture path by different models [4–7]. A recent study of the sensitivity of r-process calculations to individual nuclear properties shows importance of β-decay properties of ^{85}Ga in some astrophysical conditions [7].

II. EXPERIMENTAL TECHNIQUE

The experiment was performed at the Holifield Radioactive Ion Beam Facility (HRIBF) at Oak Ridge National Laboratory. The HRIBF [8] was an isotope separation on-line (ISOL) facility, where a 50 MeV proton beam with an average intensity of 15 μA was used to induce fission in a UC$_x$ target. Ions of ^{86}Ga were extracted from the resonant ionization laser ion source (RILIS), utilizing a two-step ionization scheme [9], accelerated to 200 keV kinetic energy, and mass analyzed by a two-stage mass separator having mass resolving powers $M/\Delta M$ of 1000 and 10 000, respectively.

The pure ^{85}Ga beam was transmitted to the Low-energy Radioactive Ion Beam Spectroscopy Station (LeRIBSS). We compared the γ rays with those obtained using the Electron Beam Plasma Ion Source in previous experiments [10–12]. We did not observe any impurities for the ^{83,85,86}Ga settings of the separator when the RILIS was used.

The LeRIBSS station was equipped with a moving tape collector (MTC), two high-purity germanium clover detectors, two plastic β detectors, and 48 ^{3}He ionization chambers for neutron detection. The neutron counters, containing in total about 600 liters of ^{3}He, were mounted in a thermalizing high-density polyethylene (HDPE) support with a 1-mm-thick cadmium outer shielding. The detection of neutrons in the ^{3}He counters is based on a capture reaction, therefore the neutron-neutron coincidences cannot be triggered by the same particle. The beam was implanted into the tape positioned at the center of the setup. The measurement cycle consisted of 2 s activity buildup, 1 s decay with no beam on, and a 0.775 s tape transport that moved the irradiated spot into a chamber located behind 5 cm of lead shielding. This cycle was repeated throughout the whole experiment. The data presented here were collected during 24 hours of beam time.

The germanium detector efficiencies were determined with standard γ-ray calibration sources. The efficiencies of β [ε_β = 40(10)%] and neutron counters [ε_n = 10(2)%], were found from comparison between the on-line γ-ray data gated and not gated by the β and neutron detectors. The correlation window for the neutron detectors was set to 100 μs, due to the slow thermalization process. For the γ-γ and γ-β coincidences a 200 ns window was used.

The readout of the detection system, including MTC logic signals, was based on XIA Pixie16 Rev. F digital electronics modules [13]. The acquisition system was operated without a master trigger, and all events were recorded independently and time-stamped with a 250 MHz clock synchronized across all modules. This allowed for the detailed off-line analysis of the data, including event-by-event analysis.

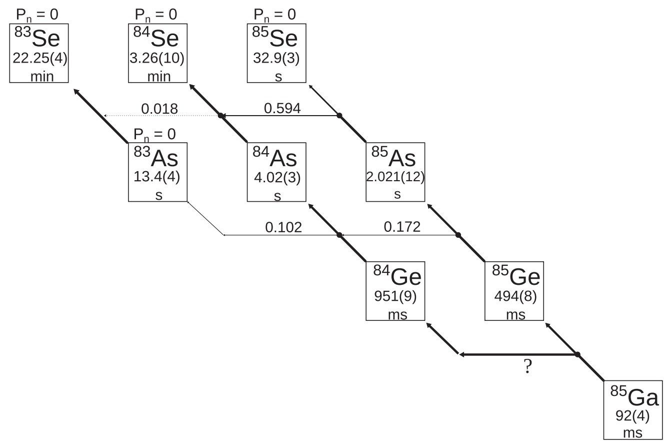

FIG. 1. Network of isotopes connected by β and β-n decays observed in experiment and/or used in calculations. Numbers above horizontal arrows indicate experimental P_n values.

III. RESULTS AND DISCUSSION

Due to the exceptional selectivity of the RILIS source combined with the high resolution of mass separation, the beam consisted of ^{85}Ga and its decay daughters only (see Fig. 1). In Fig. 2 the total β-gated and β-neutron-gated γ-ray spectra obtained in experiment are shown. With the exception of two lines (858 and 1128 keV), all transitions were identified. The identification was based on two methods: half-life measurements, and coincidences with already identified lines. The grow-in/decay-out pattern for ^{85}Ga and all of its decay daughters was easy to recognize, as presented in Fig. 3 for several lines. The solid lines show the solutions of the Bateman equation for the first [^{85}Ga, $T_{1/2} = 92(4)$ ms], second [^{84,85}Ge, $T_{1/2}$ = 951(9) and 494(8) ms respectively], or third [^{84}As, $T_{1/2}$ = 4.02(3) s] isotope in the radioactive chain (see also Fig. 1). All curves were calculated using known half-lives [2] of the isotopes, detectors, and cycle efficiencies. The only fitted parameter was the implantation rate of ^{85}Ga ions yielding 7.4(4) ions per second.

For weaker lines, when the half-life based on a fit was burdened with a large uncertainty, a ratio of the number of counts in the decay-out part of the cycle to the total number of counts was calculated. Based on the network of isotopes connected by β and $\beta-n$ decays (see Fig. 1), their half-lives and P_n values, and Bateman equations, we calculated the theoretical values for these ratios (parent is indicated in parentheses): 0.067 (^{85}Ga), 0.329 (^{85}Ge), 0.410 (^{84}Ge), 0.596 (^{85}As), 0.612 (^{84}As), and 0.663 (^{83}As).

Based on these, using β-γ spectra, we found that the 773 keV line, previously assigned to the decay of ^{84}As [12], with ratio of 0.073(17), should be placed in the decay scheme of ^{85}Ga. Similarly, two previously unknown lines at 1589 and 1797 keV, with ratios of 0.067(21), and 0.17(9) respectively, were also assigned to this decay. The 1797 keV line was found in coincidence with neutrons and with the 624 keV γ ray, which allowed us to place this transition in ^{84}Ge. The 1589 keV line was not in coincidence with neutrons, nor γ rays, thus it was placed in ^{85}Ge.

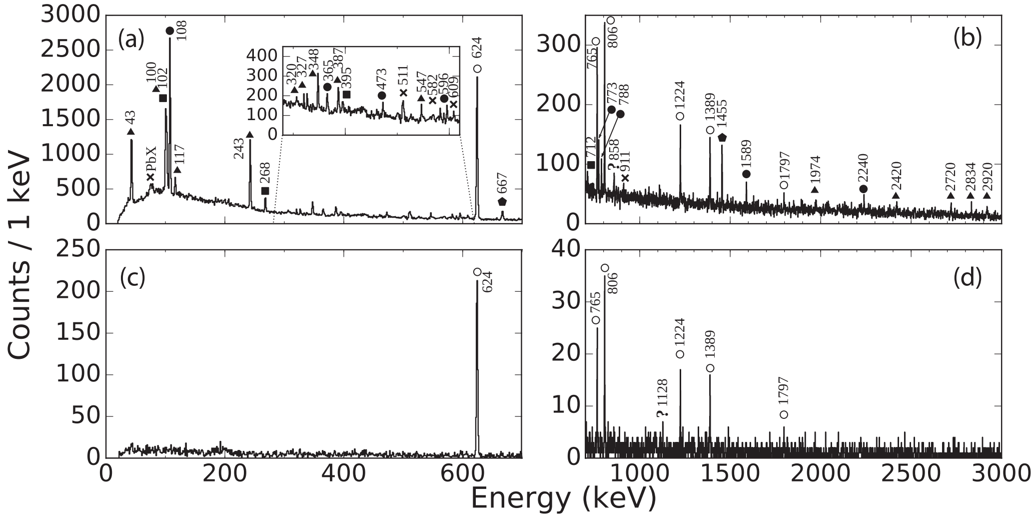

FIG. 2. (a) Range 0–700 keV and (b) range 700–3000 keV β-gated γ-ray spectra, and (c) range 0–700 keV and (d) range 700–3000 keV $\beta-n$-gated γ-ray spectra obtained in the experiment. Transitions marked by circles are assigned to the decay of ^{85}Ga (closed for β decays, and open for βn). Other transitions are marked by parent decay: squares (^{85}Ge), triangles (^{84}Ge), pentagons (^{84}As), crosses for background γ rays, and question marks for unassigned transitions.

The 858 keV γ ray was previously tentatively assigned to the $\beta-n$ branch of ^{85}Ga decay [12]. In this work we found that the ratio for this line of 0.127(32) confirms its source from the decay of ^{85}Ga. However, the coincidence with the 806 keV line is not clear, and there is no evidence for coincidence with neutrons. As a result the placement of this line is not clear, and it was not included in the decay scheme. A summary of all γ rays assigned to the decay of ^{85}Ga is shown in Table I. Uncertainties of intensities of lines are mainly due to statistical errors related to the number of counts observed.

Even though the incoming beam was isotopically pure, a number of daughter activities were seen in the collected data (cf. Fig. 2). The network of nuclides connected by β and βn decays is presented in Fig. 1. All the half-lives and delayed neutron emission probabilities, except those of ^{85}Ga, are experimentally known [2]. Therefore, it is possible to calculate the expected shape of the curve describing the number of detected neutrons versus the cycle time, with two free parameters: the ^{85}Ga P_n and the total intensity. Such calculations are shown in Fig. 4(a), where the shapes for three different P_n values are shown. Figure 4(b) presents the reduced χ^2 calculated for P_n values between 50% and 90%. Based on the reduced χ^2 calculation, the experimental P_n value is determined to be $70 \pm 5\%$.

Since the two-neutron separation energy of ^{85}Ge (8.29 MeV) is smaller than the ^{85}Ga Q_β (10.066 MeV),

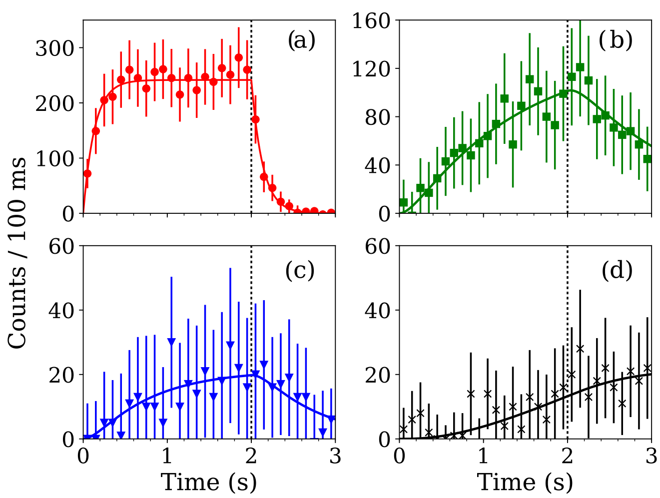

FIG. 3. The grow-in/decay-out pattern of selected γ transitions. (a) 624 keV (from decay of ^{85}Ga), (b) 242 keV (^{84}Ge), (c) 268 keV (^{85}Ge), and (d) 1455 keV (^{84}As).

TABLE I. Summary of γ rays assigned to the decay of ^{85}Ga. Intensities are given per 100 decays. Weak or uncertain γ-γ coincidences are given in parentheses.

Energy (keV)	I_γ	γ-γ
	β	
107.7(2)	12(3)	365, 596, 788
365.4(2)	1.1(3)	108
472.6(2)	0.7(2)	
595.8(2)	1.1(3)	108
773.2(2)	2.0(5)	
788.5(2)	1.4(4)	108
1589.4(2)	1.8(5)	
2240.5(4)	1.5(5)	108
	β-n	
624.2(2)	40(9)	765, 806, 1224, 1797, (2275)
764.7(2)	6.0(14)	624
805.8(2)	8.8(20)	624, (858)
858.2(2)[a]	1.4(4)	(806)
1224.3(2)	4.8(10)	624
1388.6(2)	5.5(13)	
1797.4(2)	1.3(4)	624

[a]Not placed in the decay scheme.

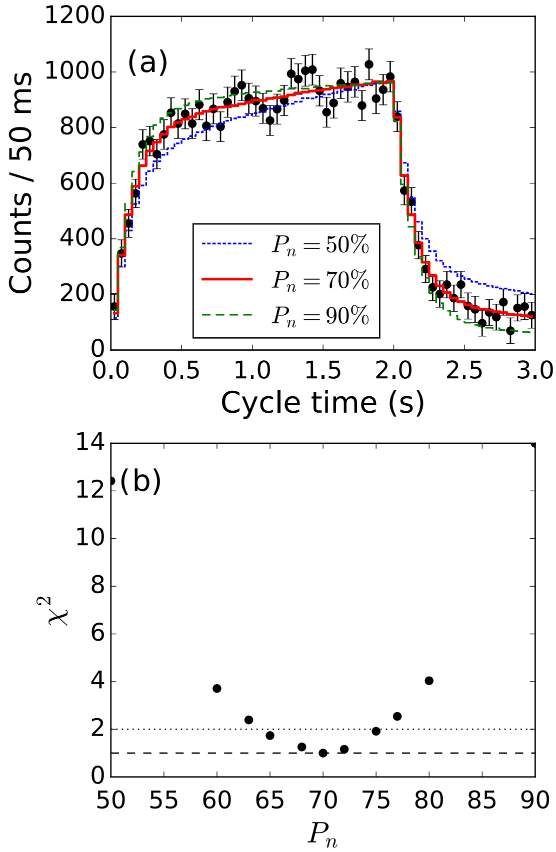

FIG. 4. (a) Experimental number of detected neutrons versus cycle time is presented with black circles. The curves were calculated using the network of isotopes presented in Fig. 1, with assumption of three different ^{85}Ga P_n values. (b) Reduced χ^2 calculated between experimental and theoretical curves [see panel (a)] for different values of ^{85}Ga P_n.

β-delayed two-neutron emission is in principle possible for this decay. However, we did not observe experimental evidence of this process. The γ spectra contains no visible transitions in the $\beta 2n$ daughter (^{83}Ge). The number of events of simultaneous detection of two neutrons in the neutron counter tubes is statistically consistent with an expected number of random coincidences. The upper limit of P_{2n} based on that value was found to be 0.1%.

It is worth noticing that the same method of P_n determination, based on calculation with a network of nuclides, was used in our previous experiment where decay of ^{86}Ga was measured [3]. Due to the limited length of the Letter it was not possible to describe details there. A distinct difference between the two experiments is that, in the ^{86}Ga case, three P_n values remained unknown (the P_n, P_{2n} of ^{86}Ga, and P_n of ^{86}Ge). In order to present the sensitivity of the method used in cases when more than one parameter in the network is unknown, we calculate here simultaneously the P_n of both ^{85}Ga and ^{85}Ge. The latter value was previously known from only one measurement [14], but it was recently remeasured and established to be 17.2(18)% [15]. In our case the fit yielded $P_n(^{85}\mathrm{Ga}) = 70(5)\%$ and $P_n(^{85}\mathrm{Ge}) = 15(5)\%$ (cf. Fig. 5), with a very well defined global minimum. This very good agreement with both the literature

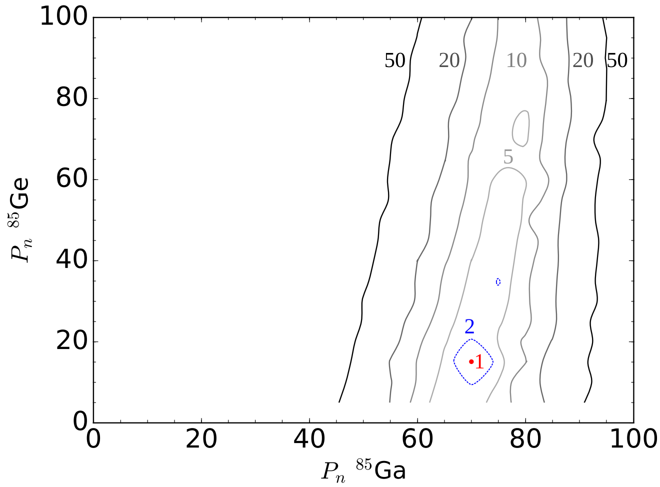

FIG. 5. Map of reduced χ^2 calculated for P_n values for both ^{85}Ga and ^{85}Ge.

data and the fit with one free P_n shows robustness of the method also in more complicated cases.

Our result completes the measurements of the P_n value for the chain of isotopes $^{79-86}$Ga. For ^{84}Ga a weighted average of

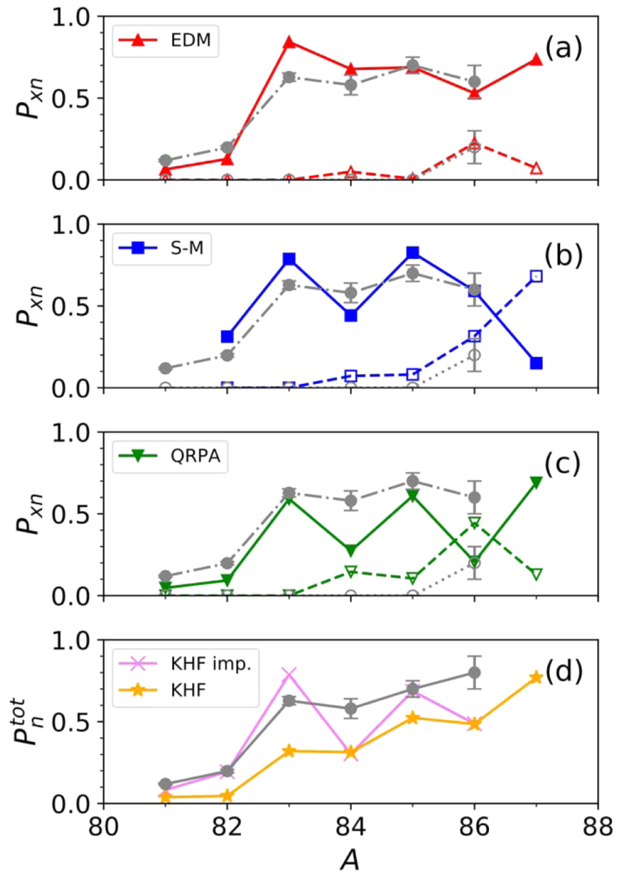

FIG. 6. P_{xn} values for the chain of Ga isotopes. Solid symbols are for P_{1n} [total P_n in panel (d)] and open ones for P_{2n}. Experimental values are shown by circles in each panel, other symbols are for theoretical calulations: (a) effective density model [19], (b) shell-model [16], (c) QRPA [18], (d) Kratz-Hermann formula [20] (stars), and improved Kratz-Hermann formula [21] (crosses).

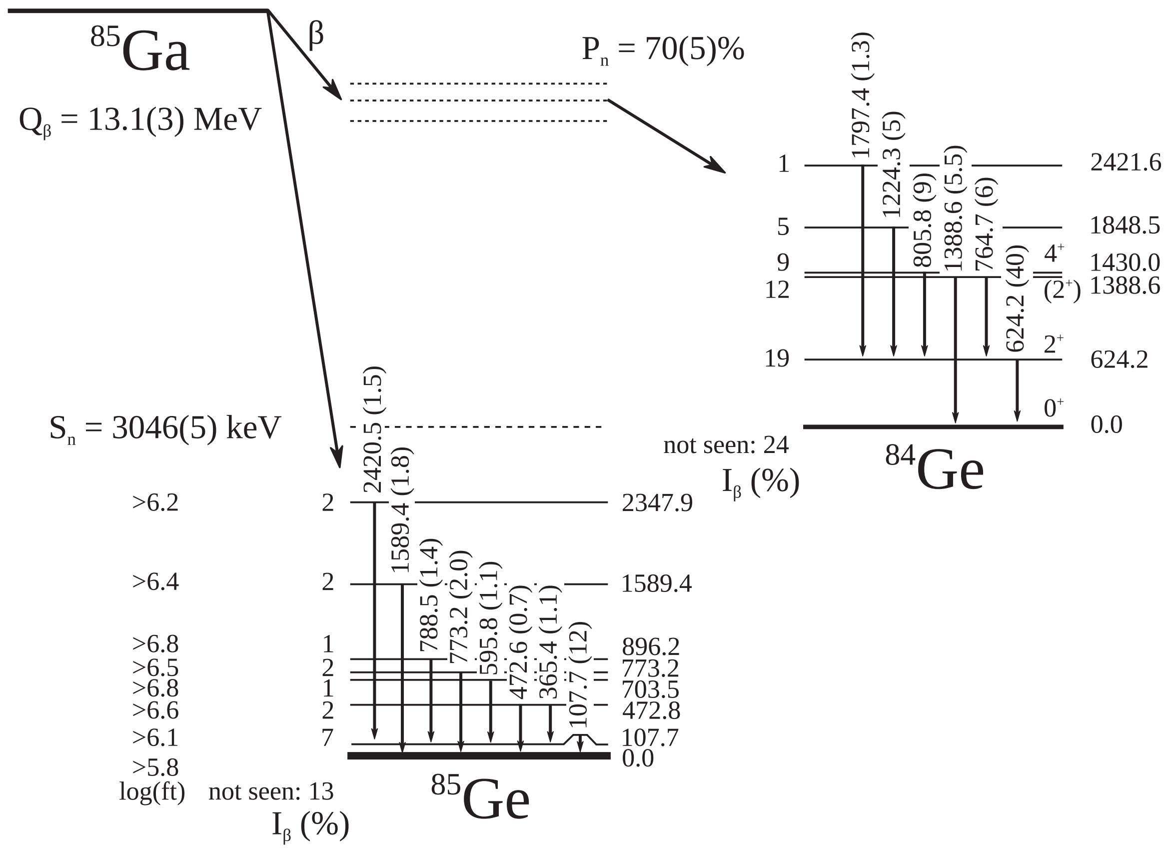

FIG. 7. Experimental β-decay scheme of ^{85}Ga. Intensities of γ transitions (in parentheses) are given per 100 parent decays. Notice that 13% of β decays and 24% of β-n decays were not seen in coincidence with γ-ray emission and are not placed in the scheme.

three available measurements is shown [10,16,17], yielding 74(14)%, 40(7)%, and 53(20)% respectively. The source of these discrepancies is not clear, however, since in ^{84}Ga a low-lying isomeric state is expected and the measured P_n values might be in fact a mixture with different content of isomeric and ground state. These experimental results are compared with several available theoretical predictions in Fig. 6. The models included are both microscopic (shell-model [16] and QRPA [18]) as well as phenomenological (effective density model [19], Kratz-Hermann formula [20], and improved Kratz-Herman formula by McCutchan *et al.* [21]). Notice that the latter two models are able to predict only the total neutron emission probabilities (i.e. the sum of probability of emission of one or more neutrons). The prediction of the effective density model for P_{2n} of ^{85}Ga is 0.7% [22], the shell model yields 8.1%, while the QRPA result is 10.5%. The shell model and QRPA use a cutoff method for estimation of P_{2n}, and the given values should be therefore treated as a upper limits. Nevertheless, all values are clearly excluded by the experimental result ($P_{2n} < 0.1\%$).

The best description of P_n values of gallium isotopes, including the ^{85}Ga case, is offered by the effective density model [19] and the shell-model with jj44bpn interaction [16]. The latter approach is able to give some more insight into nuclear structure in this region, as pointed out in a recent Letter by Madurga *et al.* [16], where experimental evidence of strong Gamow-Teller β strength located above S_n was found in the case of ^{83,84}Ga, and was well explained by the calculations. A more detailed comparison with this model will be presented in the next part of this contribution.

Based on the known efficiency of the neutron detectors, and measured P_n value, we were able to calculate the absolute intensities of the observed γ rays assigned to the decay of ^{85}Ga. This information is summarized in Fig. 7, where a decay scheme is presented. It is worth noticing that for 13% of the β decays and 24% of the βn decays no γ rays were detected. This means that they might either directly proceed to the ground state of ^{85}Ge and ^{84}Ge, respectively, or to some states deexciting by a number of weak, undetected γ-ray transitions.

In all cases of β transitions without neutron emission the calculated lower limits for the log(ft) values point to forbidden-type decays. The main part of the strength function is therefore located above the S_n threshold and results in a relatively large P_n value. This property is illustrated in Fig. 8, where a cumulative strength distribution is plotted for ^{85}Ga. The lower limit was obtained by subtracting the missing feeding separately for each observed state. The higher limit was calculated using the missing intensity (separately above and below the neutron separation energy), and by adding its value to each 100 keV bin used in the histogram. The experimental result is compared with the shell-model predictions using jj44bpn interactions including both Gamow-Teller and first-forbidden transitions [16] (Fig. 8).

It is worth noticing that the spin and parity of the ^{85}Ga ground state must be of negative parity due to unpaired proton in the f or p orbitals from the fpg shell. At the same

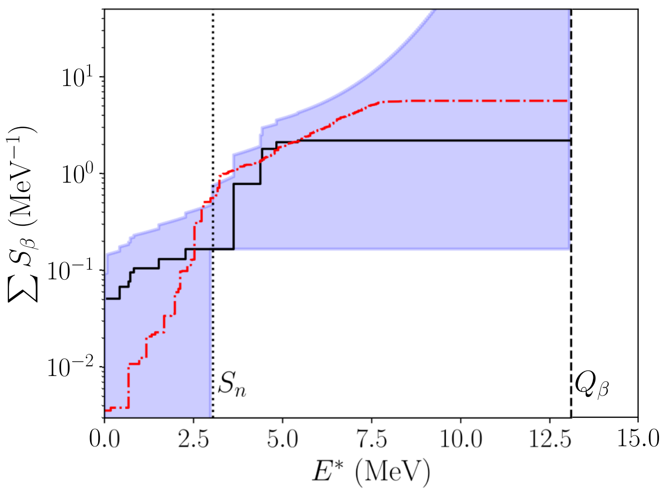

FIG. 8. Experimental limits for the cumulative strength function for ^{85}Ga. The band shows the experimental limits. Solid line: strength derived from apparent feeding; dash-dotted line: predictions of the shell model [16]. (See text for more details.)

time, the J^π of the ^{85}Ge ground state is of positive parity, coming from neutrons occupying the $d_{5/2}$ orbital. Therefore it is expected that the missing strength in the lower part of the spectrum, below S_n, is most likely shifted towards the threshold compared to the apparent feeding. This is due to the fact that direct transitions to the ground state are of forbidden type, while allowed transitions are expected near or above the threshold, and, in some part, may deexcite by γ transitions (also successfully competing with neutron emission [23,24]). On the other hand, in the upper part of the spectrum, the experimental results are expected to be close to the apparent feeding. In the case of neutron emission the parity change does not play such an important role, and direct transitions to the $\beta-n$ daughter ground state might be a significant part of the spectrum. This is well reflected in the shell-model calculations, and the overall result is not only within the experimental bands, but also goes along with the expectations.

The agreement between experimental result and calculations confirms that the relevant configurations spaces are included in the interaction (i.e., $f_{5/2}$, $p_{1/2}$, $p_{3/2}$, and $g_{9/2}$ for both protons and neutrons plus $d_{5/2}$ for neutrons), and shows that the large P_n value for ^{85}Ga is a result of a concentrated Gamow-Teller β strength, due to transformations of the ^{78}Ni core neutrons from the fpg shell into mirror protons above $Z = 28$ (cf. Fig. 9). Such transitions lead to states located in the neutron emission window. The lower part of the spectrum is a result of much weaker parity-changing forbidden transitions of $d_{5/2}$ neutrons into fp protons. The mechanism is basically the same as in the case of ^{83,84}Ga [16]. Similar conclusions were also shown in another recent study in this region ($^{82-84}$Ga) [17].

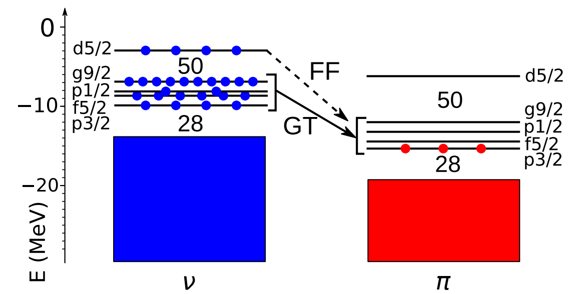

FIG. 9. Schematic view of the ^{85}Ga decay. The energies of the single particle levels were calculated with a Woods-Saxon potential with universal parametrization [25].

IV. SUMMARY

A detailed β-decay study of ^{85}Ga was performed by means of a hybrid β-γ-neutron detector suite. Thanks to the exceptional purity of the beam, the β-delayed neutron emission probability and absolute γ-ray intensities were measured for the first time. In total, eight γ transitions were assigned to the $\beta-0n$ branch and seven to the $\beta-n$ branch. Several corrections to the decay scheme were proposed, and experimental limits for the cumulative strength function were calculated. The result was compared in detail with shell-model calculations showing that, in the case of $^{83-85}$Ga, their properties might be well explained using the jj44bpn interaction. The delayed neutron emission probability was established as 70(5)%, and, also for the first time, the experimental upper limit for a potentially possible $\beta 2n$ decay was found to be 0.1%. The P_n value is relatively well described by most of the available models; however, the calculated P_{2n} are excluded by the experimental result showing that the models overestimate this decay branch in ^{85}Ga. This result should be taken into account in calculations of the r process.

ACKNOWLEDGMENTS

We would like to thank the HRIBF operations staff for the production of exceptional radioactive ion beams and for assisting with the experiments. The research of K.M. was partially performed with support from a Eugene P. Wigner Fellowship at the Oak Ridge National Laboratory, managed by UT-Battelle, LLC, for the U.S. Department of Energy under Contract No. DE-AC05-00OR22725. This work was supported by the Polish National Science Center under Contract No. UMO-2015/18/E/ST2/00217 and by the Office of Nuclear Physics, U. S. Department of Energy under Contracts No. DE-AC05-00OR22725 (ORNL), No. DE-FG02-96ER40983 (UTK), No. DE-FG-05-88ER40407, No. DE-SC00-144448 (MSU), No. DE-AC05-06OR23100 (ORAU), and No. DE-AC02-05CH11231 (UC), and by National Nuclear Security Administration under the Stewardship Science Academic Alliances program through DOE Award No. DE-NA0002132.

[1] J. Hardy *et al.*, Nucl. Phys. A **305**, 15 (1978).
[2] G. Audi, F. Kondev, M. Wang, W. Huang, and S. Naimi, Chin. Phys. C **41**, 030001 (2017).
[3] K. Miernik, K. P. Rykaczewski, C. J. Gross, R. Grzywacz, M. Madurga, D. Miller, J. C. Batchelder, I. N. Borzov, N. T. Brewer, C. Jost, A. Korgul, C. Mazzocchi, A. J. Mendez, II,

Y. Liu, S. V. Paulauskas, D. W. Stracener, J. A. Winger, M. Wolińska-Cichocka, and E. F. Zganjar, Phys. Rev. Lett. **111**, 132502 (2013).
[4] F.-K. Thielemann, J. Metzinger, and H. Klapdor, Z. Phys. A **309**, 301 (1983).
[5] K.-L. Kratz, J.-P. Bitouzet, F.-K. Thielemann, P. Möller, and B. Pfeiffer, Astrophys J. **403**, 216 (1993).
[6] K.-L. Kratz, in *Capture Gamma-Ray Spectroscopy and Related Topics*, 12th International Symposium, September 2005, Notre Dame, Indiana, edited by A. Woehr and A. Aprahamian, AIP Conf. Proc. No. 819 (AIP, New York, 2006), p. 409.
[7] M. Mumpower, R. Surman, G. McLaughlin, and A. Aprahamian, Prog. Part. Nucl. Phys **86**, 86 (2016).
[8] J. Beene *et al.*, J. Phys. G **38**, 024002 (2011).
[9] Y. Liu *et al.*, Nuc. Instrum. Methods Phys. Res. B **298**, 5 (2013).
[10] J. A. Winger, K. P. Rykaczewski, C. J. Gross, R. Grzywacz, J. C. Batchelder, C. Goodin, J. H. Hamilton, S. V. Ilyushkin, A. Korgul, W. Królas, S. N. Liddick, C. Mazzocchi, S. Padgett, A. Piechaczek, M. M. Rajabali, D. Shapira, E. F. Zganjar, and J. Dobaczewski, Phys. Rev. C **81**, 044303 (2010).
[11] C. Mazzocchi, K. P. Rykaczewski, A. Korgul, R. Grzywacz, P. Bączyk, C. Bingham, N. T. Brewer, C. J. Gross, C. Jost, M. Karny, M. Madurga, A. J. Mendez, II, K. Miernik, D. Miller, S. Padgett, S. V. Paulauskas, D. W. Stracener, M. Wolińska-Cichocka, and I. N. Borzov, Phys. Rev. C **87**, 034315 (2013).
[12] A. Korgul, K. P. Rykaczewski, R. Grzywacz, H. Sliwinska, J. C. Batchelder, C. Bingham, I. N. Borzov, N. Brewer, L. Cartegni, A. Fijałkowska, C. J. Gross, J. H. Hamilton, C. Jost, M. Karny, W. Królas, S. Liu, C. Mazzocchi, M. Madurga, A. J. Mendez, II, K. Miernik, D. Miller, S. Padgett, S. Paulauskas, D. Shapira, D. Stracener, K. Sieja, J. A. Winger, M. Wolińska-Cichocka, and E. F. Zganjar, Phys. Rev. C **88**, 044330 (2013).
[13] http://www.xia.com/.
[14] K.-L. Kratz *et al.*, Z. Phys. A **340**, 419 (1991).
[15] J. Agramunt *et al.*, Nucl. Data Sheets **120**, 74 (2014).
[16] M. Madurga, S. V. Paulauskas, R. Grzywacz, D. Miller, D. W. Bardayan, J. C. Batchelder, N. T. Brewer, J. A. Cizewski, A. Fijałkowska, C. J. Gross, M. E. Howard, S. V. Ilyushkin, B. Manning, M. Matoš, A. J. Mendez, II, K. Miernik, S. W. Padgett, W. A. Peters, B. C. Rasco, A. Ratkiewicz, K. P. Rykaczewski, D. W. Stracener, E. H. Wang, M. Wolińska-Cichocka, and E. F. Zganjar, Phys. Rev. Lett. **117**, 092502 (2016).
[17] D. Verney, D. Testov, F. Ibrahim, Y. Penionzhkevich, B. Roussière, V. Smirnov, F. Didierjean, K. Flanagan, S. Franchoo, E. Kuznetsova, R. Li, B. Marsh, I. Matea, H. Pai, E. Sokol, I. Stefan, and D. Suzuki, Phys. Rev. C **95**, 054320 (2017).
[18] P. Möller, B. Pfeiffer, and K.-L. Kratz, Phys. Rev. C **67**, 055802 (2003).
[19] K. Miernik, Phys. Rev. C **88**, 041301(R) (2013).
[20] K.-L. Kratz and G. Herrmann, Z. Phys. A **263**, 435 (1973).
[21] E. A. McCutchan, A. A. Sonzogni, T. D. Johnson, D. Abriola, M. Birch, and B. Singh, Phys. Rev. C **86**, 041305(R) (2012).
[22] K. Miernik, Phys. Rev. C **90**, 054306 (2014).
[23] A. Gottardo *et al.*, Phys. Lett. B **772**, 359 (2017).
[24] V. Vaquero, A. Jungclaus, P. Doornenbal, K. Wimmer, A. Gargano, J. A. Tostevin, S. Chen, E. Nácher, E. Sahin, Y. Shiga, D. Steppenbeck, R. Taniuchi, Z. Y. Xu, T. Ando, H. Baba, F. L. B. Garrote, S. Franchoo, K. Hadynska-Klek, A. Kusoglu, J. Liu, T. Lokotko, S. Momiyama, T. Motobayashi, S. Nagamine, N. Nakatsuka, M. Niikura, R. Orlandi, T. Saito, H. Sakurai, P. A. Söderström, G. M. Tveten, Z. Vajta, and M. Yalcinkaya, Phys. Rev. Lett. **118**, 202502 (2017).
[25] S. Ćwiok *et al.*, Comput. Phys. Commun. **46**, 379 (1987).